



## Attenuation of acoustic resonances in an inclined open cavity using Micro Perforated Panels

Cristobal GONZALEZ DIAZ<sup>1</sup>; Santiago ORTIZ<sup>2</sup>; Pedro COBO<sup>3</sup>

<sup>1,2,3</sup> Instituto de Tecnologías Físicas y de la información (ITEFI)

Consejo Superior de Investigaciones Científicas (CSIC)

Serrano 144, 28006 Madrid (SPAIN)

### ABSTRACT

Airframe noise is equal to or louder than engine noise during the landing approach of a commercial aircraft. Cavity noise is one of the most important airframe noises. When airflow passes over an open cavity, due to vortex shedding at the upstream edge of the cavity and the geometry of the cavity, high-level aero-acoustic noise may be generated. When the incident acoustic waves produced by the airflow couples with the acoustic cavity resonances intensive tones are generated in and around the cavity at resonant discrete frequencies. Sound radiation due to the acoustic cavity resonances in an open cavity could be achieved by passive means such as lining the walls with absorbent materials. Porous and fibrous materials are used where there is no airflow. However, in presence of airflow, Micro Perforated Panels (MPP) and Porous metals are employed instead. This paper presents experimental and simulated results of the attenuation of acoustic cavity resonance tones in and around of an open cavity without and with inclined walls with lined Micro Perforated Panels.

Keywords: Micro Perforated Panels (MPP), cavity resonances.

I-INCE Classification of Subjects Number(s): 21.6.9, 32.1.

### 1. INTRODUCTION

Airframe noises are generated by the interaction between the vortex streets in the turbulent wake or between the vortices and the solid body edge(s). The phenomena are further complicated by a possible aero-acoustic feedback loop or a possible Helmholtz fluid resonance. Cavity noise is one of the most important airframe noises (1, 2). When flow passes over a cavity or opening, due to vortex shedding at the upstream edge of the cavity, intensive tone noises may be generated. Strong tonal oscillations occur in a feedback loop between the two edges of the cavity opening. First, the vortices generated and shed from the upstream edge of the cavity convect downstream, impinge on the other edge, and produce acoustic waves. Then, as the acoustic waves propagate either inside or outside of the cavity to the upstream edge, where receptivity of the wall jet shear layer is high, a new instability wave (vortex) is stimulated and shed, a feedback cycle is thus completed. The tone noise generated in this way may be categorized as fluid-dynamic oscillation noise. Most high-speed flow (supersonic, transonic, or high subsonic flows) noises are generated by the fluid dynamic feedback oscillation mode. However, at low flow speed (1), depending on the geometry of the cavity, another type of tone noise due to fluid resonant oscillation within the cavity may occur. The sound waves inside the cavity may be longitudinal or transverse depending on the aspect ratio of the cavity. For a deep cavity at low flow speed, both major tone noise-generating mechanisms may coexist. If one or more walls of a cavity undergo displacement that is large enough to exert feedback control on the shear layer perturbations during the cavity oscillation, the excitation is defined as fluid elastic. The vibrating structure has the same function as the resonating wave in a fluid resonant oscillation. A

---

<sup>1</sup> cristobal.g.diaz@csic.es

<sup>2</sup> santiago.ortiz@caend.upm-csic.es

<sup>3</sup> pedro.cobo@csic.es

resonant type process is used to amplify the perturbed shear layer flow. Wheel wells and Auxiliary Power Unit compartments are sources of high level cavity tones during the airplane landing and take off operations. Several researches have reported numerical methods to provide the eigenvalues (resonances frequencies) and eigenfunctions (normal modes) of open cavities without flow. Koch (3) proposed to find the acoustic resonances of 2D and 3D rectangular open cavities by solving Helmholtz wave equation by finite-element methods (FEM). Ortiz et al. (4) suggested the use of the Image Source Model (ISM) to obtain the impulse response of an open cavity. This method gives the acoustic resonances of a 3D open cavity by a fast and efficient method, which models the time response at any point in the medium as the convolution of the source waveform with the impulse response of the cavity. The peaks of the FRF were identified then as the resonance frequencies of the open cavity. The proposed ISM method was experimentally validated on a 3D cubic open cavity made with medium density fibreboard panels of thickness 3 cm and dimensions  $(W, L, D) = (53, 32, 38)$  cm.

The acoustic resonances in the open cavity can be attenuated by noise control techniques. One passive control technique consists of lining the inner walls of the cavity with absorbing material. Whilst porous materials provide wideband absorption, they are discouraged in presence of air-flow. Since open cavity tones are usually driven by air flow (wheel wells in airplanes, shallow cavity above bogies in trains, sunroof in cars), alternative absorbers supporting air flowing might be used. Micro-Perforated Panels (MPP) are recognized as the next generation absorbing materials. Furthermore, they can be used in presence of air flow (5). Their absorption curve can be reliably predicted by means of models, which depend on the constitutive parameters of the MPP.

The main shortcoming of constructing MPP absorbers, its high manufacturing cost, can be currently avoided by using the infiltration technique proposed by Cobo and Montero de Espinosa (6). This technique consists of mixing common salt grains of controlled size and quantity with a commercial epoxy resin. When the mixture cures, the sample is introduced into a water tank to dissolve the salt grains, appearing the holes with the shape and size of the salt grains.

The major aim of this work is to report the attenuation of resonant tones in a cubic open cavity when its inner walls are lined with MPPs manufactured by infiltration, using a point source. The open cavity will be described in Sec. 2. The MPPs used to line the inner walls of the cavity will be analysed in Sec. 3. The numerical procedure and the experimental and numerical results will be explained in Sec. 4 and 5, respectively. Finally, the main conclusions will be disclosed in Sec. 6.

## 2. THE OPEN CAVITY

A cubic 3D open cavity was made with DM wood panels of 3 cm thickness. The open cavity shown in Figure 1a, has inner dimensions  $(W, L, D) = (53, 32, 38)$  cm. A wooden panel was inserted around the open wall of the cavity to avoid back radiation between the source and the measurement points. The former Sonavox Honeycomb loudspeaker (4") set at the centre line of the front wall was substituted by a point source described in (7). This is the open cavity whose acoustic resonances were previously characterized by Ortiz et al. (4, 7). The inner walls of this cavity will be lined with the MPP absorbers described in Sec. 3. The open cavity lined with MPPs is shown in Figure 1b.

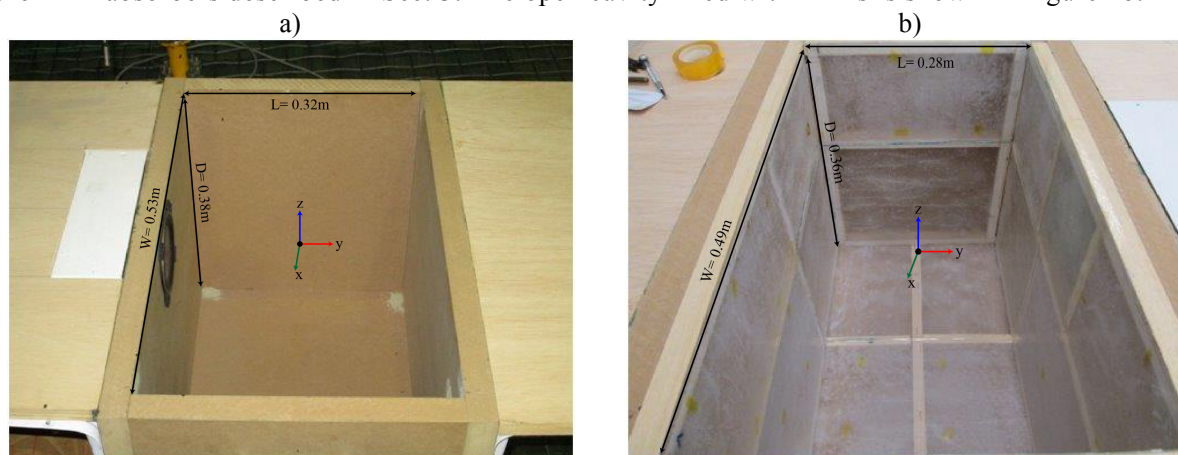


Figure 1 – a) Open cavity and b) open cavity lined with MPPs. The coordinate axis origin is at the centre of the cavity.

### 3. The Micro Perforated Panel

A Micro Perforated Panel (MPP) is a panel of thickness  $t$ , with perforations of diameter  $d$ , porosity  $\phi$  in front of an impervious wall at a distance  $D$ .

Several models have been proposed to predict the absorption of MPPs. The pioneer work of Maa (8, 9) modelled the input impedance of the MPP including three terms: that of the holes, that of the edges, and the one corresponding to the air cavity.

Atalla and Sgard (10) proposed the equivalent fluid model to characterize the input impedance of an MPP. This model uses the following equation for the input impedance:

$$Z_{AS} = i\omega\rho_0\alpha_\infty \left( 1 + \frac{\sigma\phi}{i\omega\rho_0\alpha_\infty} \sqrt{1 + i \frac{4\omega\rho_0\mu\alpha_\infty^2}{\sigma^2\phi^2r^2}} \right) \frac{t}{\phi} - iZ_0 \cot(kD), \quad (1)$$

where  $\omega$  is the angular frequency,  $\rho_0$  is the air density,  $\mu$  is the air viscosity,  $r=d/2$  is the hole radius,  $k=\omega/c$  is the wavenumber,

$$\alpha_\infty = 1 + \frac{2\varepsilon_e}{t}, \quad (2)$$

is the geometrical tortuosity,

$$\varepsilon_e = 0.48\sqrt{\pi r^2} (1 - 1.14\sqrt{\sigma}), \quad (3)$$

is the excess of vibrating mass at the hole edges, and

$$\sigma = \frac{32\mu}{\phi d^2}, \quad (4)$$

is the flow resistivity.

Both models yield very similar values for the input impedance of a MPP. In this paper the equivalent fluid model proposed by Atalla and Sgard will be used.

One of the main disadvantages to construct an MPP is its high manufacturing cost. Cobo and Montero de Espinosa (6) proposed an infiltration technique to manufacture cheaper MPPs. The procedure is simpler if  $d=t$ . The MPPs manufactured by infiltration contain irregular, unevenly distributed perforations. Cobo and Montero de Espinosa demonstrated that the equations of the Maa and equivalent fluid models can be still used whenever the constitutive parameters are slightly modified. For instance, the equivalent fluid model for a MPP manufactured by infiltration requires modified values for the flow resistivity and geometrical tortuosity given by (6)

$$\sigma = s_\sigma \frac{32\mu}{\phi d^2}, \quad (5)$$

$$\alpha_\infty = s_{\alpha_\infty} \left( 1 + \frac{2\varepsilon_e}{t} \right), \quad (6)$$

where  $s_\sigma$  and  $s_{\alpha_\infty}$  are real numbers close to 1. The modified equivalent fluid model has been used to design MPPs for lining the inner walls of the open cavity. Two MPPs were designed to cover the frequency range between roughly 700 and 2000 Hz.

The proposed MPPs have the parameters summarized in Table 1. Figure 2 shows the normal incidence absorption curves for both MPPs with  $D = 2$  cm and  $s_\sigma = 1.4$  and  $s_{\alpha_\infty} = 0.7$ . The maximum absorption provided by MPP1 and MPP2, is at 940 Hz and 1100 Hz, respectively.

Then, the inner walls of the open cavity described in Sec. 2 were lined with samples of both MPPs according to a patchwork pattern. The final lined cavity is shown in Figure 1b.

Table 1 – Parameters of the two proposed MPPs.

MPP	$d$ (mm)	$t$ (mm)	$\phi$ (%)
MPP1	0.55	0.55	0.50
MPP2	0.4	0.4	0.52

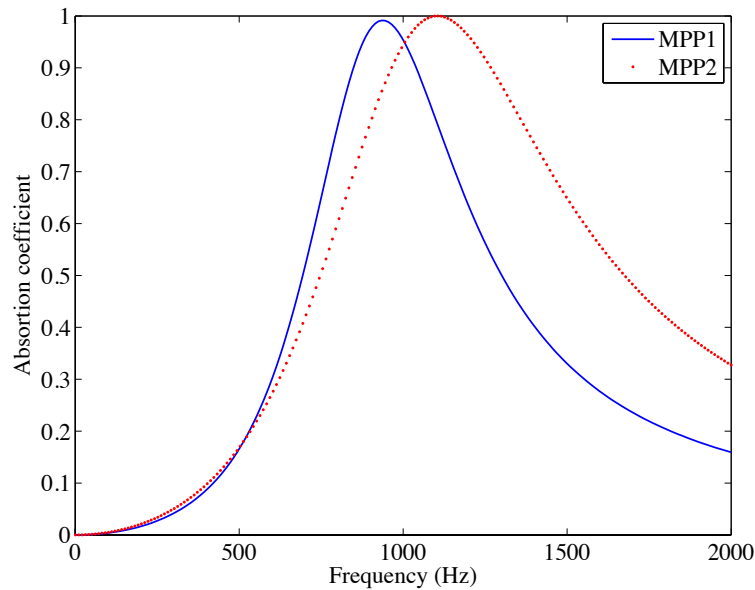


Figure 2 – Absorption coefficient of MPP1 and MPP2 with  $D=2\text{cm}$ ,  $s_o = 1.4$  and  $s_{oc}=0.7$ .

#### 4. NUMERICAL PROCEDURE – FINITE ELEMENTS ANALYSIS (FEM)

The Finite Element Method (FEM) software used is Comsol Multiphysics 4.4. The numerical model is experimentally validated by comparing the measured natural frequencies extracted from the peaks of the FRF (4) to the simulated natural frequencies extracted from Comsol. Table 3 shows the modal frequencies of the open cavity extracted from the peaks of FRF; experimentally, numerically and simulated. The selected mesh size of the model results in an acceptable balance between the frequency range of interest and the calculation time. In the performed simulation a Monopole Point Source located in the “Source Point” excites the cavity. A frequency resolution of 1 Hz and frequency range of 1-1500 Hz are chosen for the frequency domain simulations.

A Perfectly Matched Layer (PML) has been chosen to simulate the presence of an open boundary, this layer absorbs all outgoing wave energy in frequency-domain problems without any impedance mismatch—causing spurious reflections—at the boundary.

#### 5. RESULTS

Assuming a Cartesian coordinates system with origin at the centre of the cavity (see Figure 1), the source is located at  $(x_s, y_s, z_s) = (-0.195, -0.16, 0.1)$ . The impulse responses were measured at 3 points in the cavity. The coordinates in the measurements and simulations are the same. The points were chosen so that they can be accessed both with the unlined and lined cavities. The “Lower” point is placed close to the wall opposite to the wall containing the point source. The “Upper” point is set close to the lateral wall farther from the wall containing the source. Finally, the “Outer” point is located outside the cavity, above the upper baffle opposite to the wall containing the source. Table 2 summarises the coordinates of the measurement and the simulated points and the source.

Table 2 – Coordinates of the measurement/simulated points and source.

Point	X (m)	Y (m)	Z (m)
Lower	0.035	0.11	-0.14
Upper	0.185	-0.04	0.14
Outer	0.085	0.21	0.24
Source	-0.195	-0.16	0.1

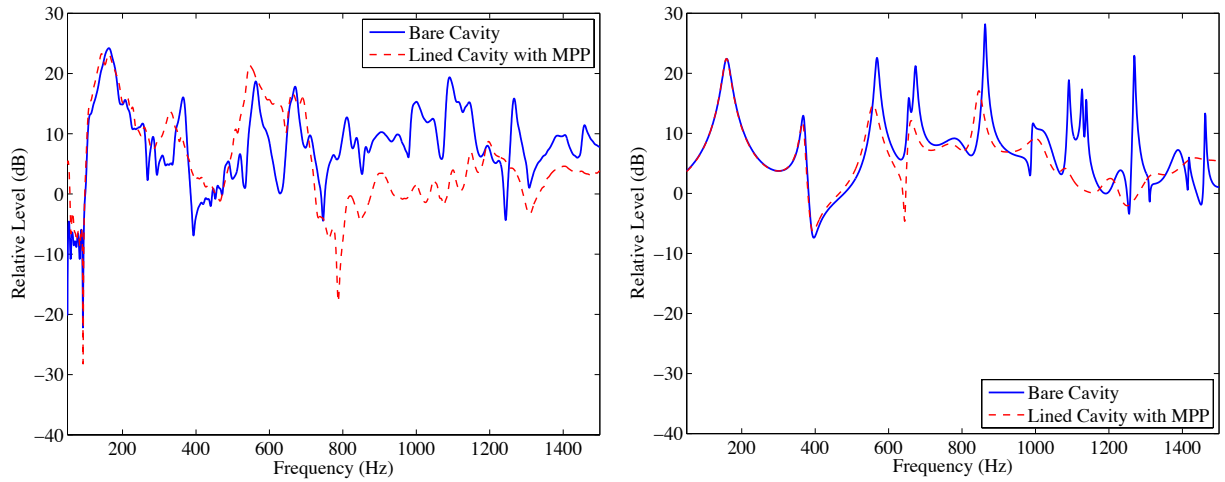


Figure 3 – a) Experimental, b) Simulated FRF with and without MPP lining at the “Lower” point of the cavity.

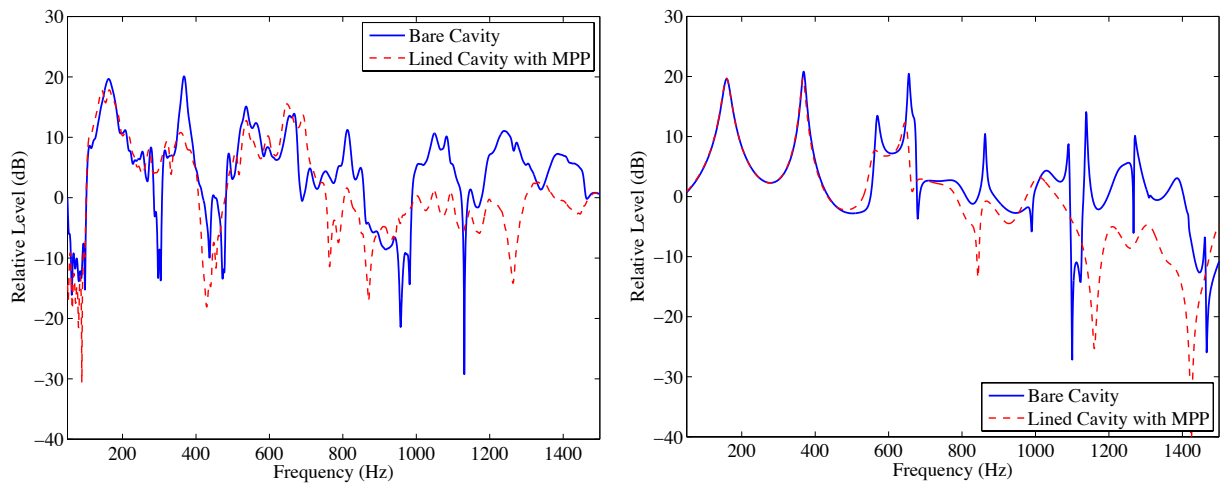


Figure 4 – a) Experimental, b) Simulated FRF with and without MPP lining at the “Upper” point of the cavity.

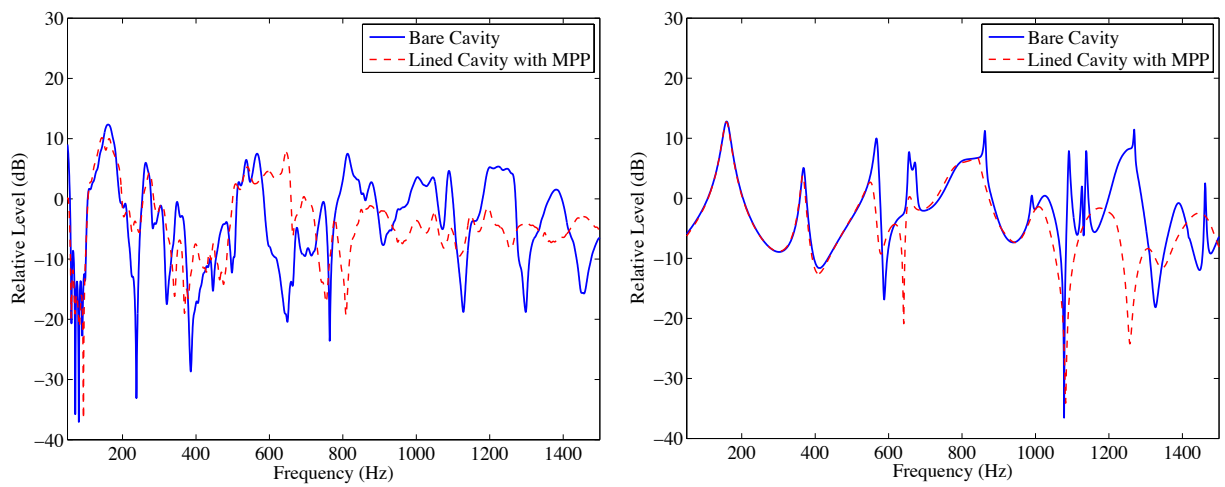


Figure 5 – a) Experimental, b) Simulated FRF with and without MPP lining at the “Outer” point of the cavity

Figures 3-5 show the FRFs at the “Lower”, “Upper” and “Outer” points with and without MPP lining. The left figures (a) are the measurements results while the right figures (b) are the simulated results. Although there is a fairly good overall agreement, simulations tend to show sharper peaks. This could be due to the fact that the absorption coefficient of the cavity walls has been assumed as “Hard Boundary Walls”.

It can be seen that the main effect of the MMP lining is to decrease 10-15 dB the level of the resonant frequencies of the cavity in the frequency range from 600-1500 Hz. At lower frequencies, the main effect of MMP lining is to shift the frequency of the resonances due to a minor change of the cavity geometry. In the “Lower” point, Figure 3, the maximum reduction (about 15 dB) is obtained around 1100 Hz. Below 600 Hz no reduction is seen. Same pattern is observed for both, experimental and simulation results. The attenuation of the peaks of the FRF at the “Upper” point, Figure 4 is lesser, as the amplitudes of the peaks are lower. However, the peaks are also decreased around 5-10 dB at the frequency range from 700 to 1400 Hz. The peak amplitudes at the “Outer” point outside the cavity, Figure 5, are even lower; this point is farther away from the source point. At this position, the MPP liner provides reductions lesser than 10 dB between 400 and 1500 Hz.

Table 3 – Modal frequencies of the open cavity extracted from the peaks of FRF. (4)

Mode	$F_{exp}(Hz)$	$F_{the}(Hz)$	$F_{num}(Hz)$
(0,0,0)	157	151.4	159
(1,0,0)	374.4	Not seen	368
(0,1,0)	575	549	569
(2,0,0)	680.9	659.8	673
(2,1,0)	863.4	854.5	863
(0,2,0)	1103	1090	1091
(2,2,0)	1290	1270	1269
(4,1,0)	1430	1431	1462
(4,2,0)	1642	1646	

Other passive control technique to attenuate the acoustic resonances of an open cavity is to change its geometry. In general, the design modification of an open cavity to decrease the sound it produces enforced design requirements limits to the design freedom. Overall open cavity dimensions are restricted due to operation of the plane (the limitation of runway loads defines number of wheels and spacing, gear locations defined by lateral stability and rotation before lift-off, brake cooling system), safety (tyre burst) and cost (weight, system complexity, maintenance). Therefore few constrains should be taking into account such as the volume, length, width, depth... of an open cavity where the landing gear should fit.

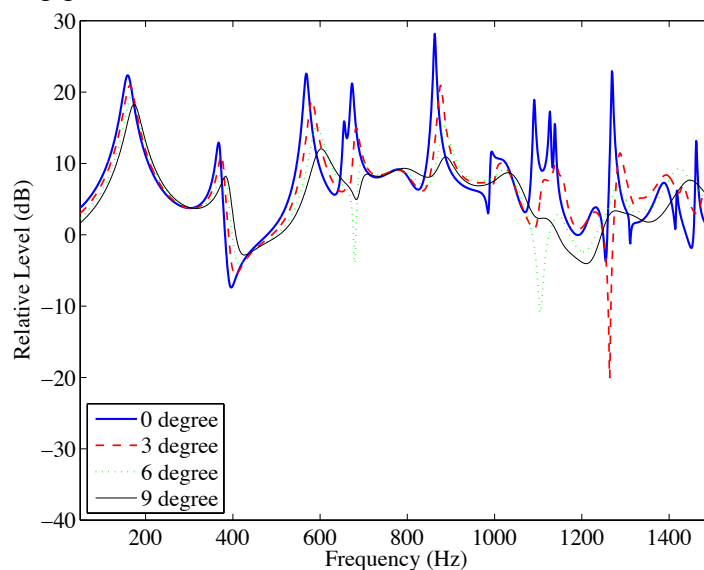


Figure 6 – Simulated FRF at the “Lower” point for different tilting angle of the walls of the cavity.

Figures 6-8 show the simulated FRF of an open cavity where the four walls of the cavity have 0,

3, 6, or 9 degree-tilting angle like the reversed pyramided with a truncate top. The dimensions of the open cavity where the walls of the cavity have 0 degree-tilting angle are the same of the open cavity described in section 2. The volume is the equal for all the four cavities. It can be seen that by tilting the walls of the cavity the resonance frequencies of the cavity are attenuated; the higher is the inclination of the wall of the cavity the larger is the attenuation of the peaks of the resonance frequencies. It can also be observed that at high frequencies, where the passive strategies are more efficient, the attenuation is higher.

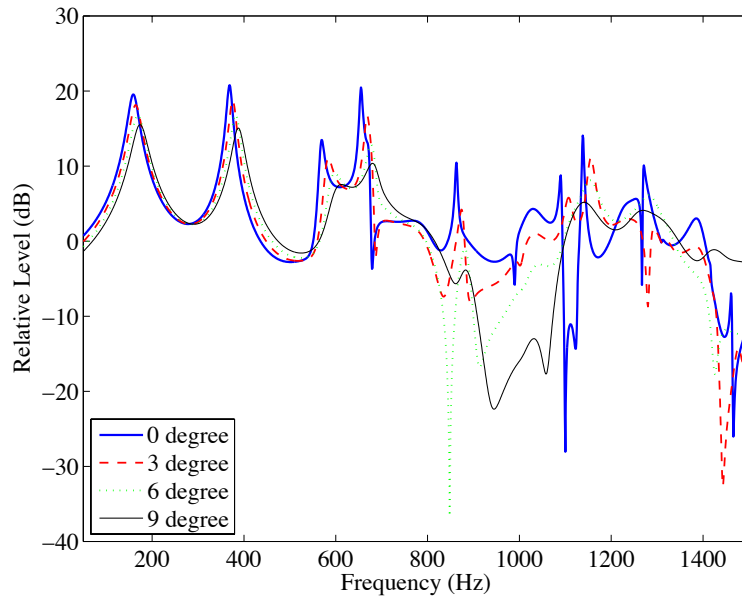


Figure 7 – Simulated FRF at the “Upper” point for different tilting angle of the walls of the cavity.

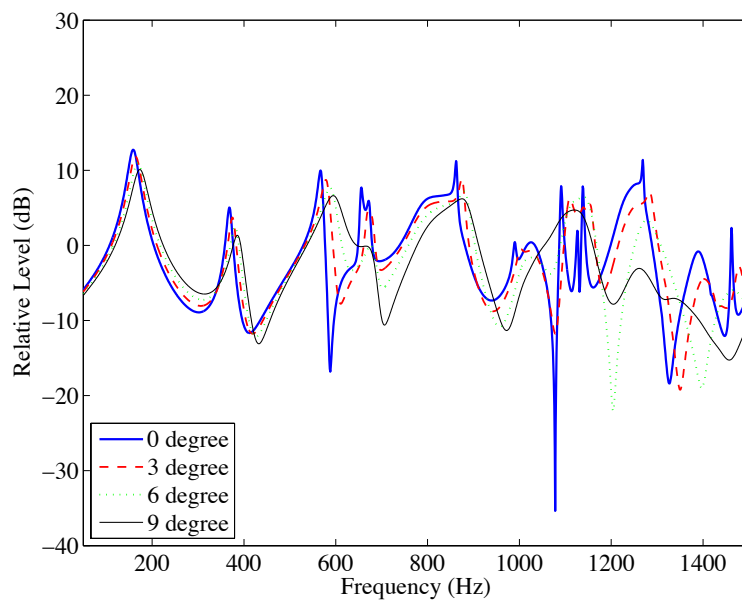


Figure 8 – Simulated FRF at the “Outer” point for different tilting angle of the walls of the cavity.

## 6. SUMMARY AND CONCLUSIONS

The effect of lining the inner wall of an open cavity with and without inclined walls in the acoustic field inside and around the cavity has been experimental and numerically validated.

A wooden open cavity constructed previously, changing the former 4" loudspeaker for an inverse filtered point source has been used for the measurements. Also, the inner walls of the cavity have been lined with MPPs manufactured by an infiltration technique. The MPPs have been designed to provide absorption in a frequency band ranging from 700 to 4500 Hz. However results in the frequency range of 1-1500 Hz are shown in this study.

The resonance frequencies of the cavity have been elucidated experimentally measuring the impulse responses between a fixed source and a microphone moving along points inside and outside the cavity. The Fourier transform of these impulse responses to the frequency domain gives the FRF functions at each measurement point. The peaks of the FRFs are then identified as the resonance frequencies of the open cavity.

The effect of lining the inner walls with MPPs is to attenuate the resonance peaks in the frequency band where the MPPs were designed to absorb sound.

Also, it has been shown the effect of tilting the four walls of an open cavity.

## ACKNOWLEDGEMENTS

The research leading to these results has received funding from the EU Seventh Framework Programme Marie Curie IEF project "ACOCTIA" (FP7-PEOPLE-2011-IEF, Grant Agreement No. 301287).

## REFERENCES

1. Rossiter.J.E. Wind-tunnel experiments on the flow over rectangular cavities at subsonic and transonic speeds. Aeronautical Research Council Reports and Memoranda, Technical report 3438. 1964.
2. Gloerfelt X. Cavity Noise. VKI Lectures: Aerodynamic noise from wall-bounded flows: Von Karman Institute; 2009.
3. Koch W. Acoustic Resonances in Rectangular Open Cavities. AIAA Journal. 2005;43(11):2342-9.
4. Ortiz S, Plenier CL, Cobo P. Efficient modeling and experimental validation of acoustic resonances in three-dimensional rectangular open cavities. Applied Acoustics. 2013;74(7):949-57.
5. Cobo P, Ruiz H, Alvarez J. Double-Layer Microperforated Panel/Porous Absorber as Liner for Anechoic Closing of the Test Section in Wind Tunnels. Acta Acustica united with Acustica. 2010;96(5):914-22.
6. Cobo P, Montero de Espinosa F. Proposal of cheap microperforated panel absorbers manufactured by infiltration. Applied Acoustics. 2013;74(9):1069-75.
7. Ortiz S, Gonzalez Diaz C, Cobo P, Montero de Espinosa F. Attenuating open cavity tones by lining its walls with microperforated panels. Noise Control Engineering Journal. 2014;62(3):145-51.
8. Maa D-Y. Potential of microperforated panel absorber. The Journal of the Acoustical Society of America. 1998;104(5):2861-6.
9. Maa D-Y. Microperforated-Panel Wideband Absorbers. Noise Control Engineering Journal. 1987;29(3):77-84.
10. Atalla N, Sgard F. Modeling of perforated plates and screens using rigid frame porous models. Journal of Sound and Vibration. 2007;303(1-2):195-208.